STUDIES OF NbTi STRANDS EXTRACTED FROM CORELESS RUTHERFORD CABLES

L. F. Goodrich, E. S. Pittman, and J. W. Ekin
National Bureau of Standards
Boulder, Colorado 80303

and

R. M. Scanlan
Lawrence Berkeley Laboratory
Berkeley, California 94720

Abstract

The electromechanical properties of NbTi strands extracted from coreless Rutherford cables were studied to clarify the relative effects of strand location and field angle on current degradation that occurs in cables that have been compacted into a keystone shape. Detailed critical-current measurements were made on two samples which were fabricated under controlled conditions. These are prototype cables for high energy physics applications. Specific factors that are addressed are the nature, location, and amount of degradation. This information is intended to lead to methods for reducing the amount of critical-current degradation in cable manufacture.

Introduction

The measurements reported here were made on two samples, denoted as Sample A (billet 5914, cable SC 305) and Sample B (billet 5212, cable SC 297). Sample A was a strand from a cable that was commonly used for cable studies late in 1985 and early 1986. Sample B was a strand from a cable that was re-rolled through the turkshead (to re-size it) after it had been cabled. This re-rolling may have been done in the direction opposite the original cabling and roll direction. The re-rolled cable Sample B was a worst-case situation that was studied to more clearly identify the degradation features. The comparison of the results of measurements on these two cables indicated significant similarities and differences. The critical current, I_c, of strands extracted from cables was measured as a function of position along the cable and magnetic field orientation. A more complete report on this work can be found in Ref. 1. Information on the cable fabrication and current density with high homogeneous NbTi alloy can be found in Refs. 2, 3 and 4.

Experimental Details

The samples were from 30-strand cables and started as 0.65-mm-diameter round wires with a right hand filament twist of about 0.8 twist/cm. The cable had a left hand lay with a 69-mm pitch and a cable width of 9.7 mm, mid-thickness of 1.17 mm, and a keystone angle of about 1.24°. Sample A had a Nb diffusion barrier on each of the 6006, 5-μm-diameter filaments. Sample B had 648, 16-μm-diameter filaments and did not have a diffusion barrier. The Sample A billet was double stacked; Sample B was single stack. The starting-wire critical currents (before the cabling process) were determined at 5 T and 4.02 K using a 0.1 μV/cm criterion (Sample A, 320 A; Sample B, 347 A). The critical-current density was calculated using the NbTi cross-sectional area (Sample A, 2500 A/mm^2; Sample B, 2900 A/mm^2), which was determined using the copper-to-superconductor volume ratio (Sample A, 1.64; Sample B, 1.77). The critical-current density at 4.22 K would be about 6% less than the values listed at 4.02 K.

A number of voltage taps were placed along the length of the strand to determine its local electrical properties after it had been deformed by the cabling process. Three regions of the cable were studied: the thin edge, the face (top or bottom), and the thick edge. Each of these regions was divided with voltage taps into three approximately equal-length, adjacent segments. The three segments of each cable edge were denoted as the central flat edge and the two corners (bent portion). These edge voltage taps had separations of 2 to 2.5 mm (thin edge) and 2.5 to 3 mm (thick edge). The voltage taps along the face of the cable had separations of about 9 mm and they did not include any of the cable corner regions. The precision and accuracy of the critical current measurements were limited by the low voltage for these closely spaced voltage taps and the fact that the sample would quench before very much voltage drop could be developed between some voltage taps. The precision was about ±1% and the accuracy was about ±2%.

The effective critical current was defined as the critical current determined by adding the voltage contributions of each strand segment, taking into account that the positions along the face need to be counted twice for one pitch length. This total voltage was then converted to an effective electric field by dividing by one pitch length. This was useful because it related more directly to measurements made on the whole cable where several pitch lengths were included between the voltage taps.

Results

The data presented here are preliminary in that they may not represent averages of a number of specimens. There is no reason to believe, however, that these two specimens were not typical. Independent measurements on the cables[5] indicated that Sample A was degraded by about 9% and had a field anisotropy of about 11% and Sample B was degraded by 22% and had an anisotropy of -11%. Anisotropy refers to 1 minus the ratio of perpendicular I_c (90°) to parellel I_c (0°) and degradation refers to 1 minus the ratio of perpendicular I_c to starting wire I_c (see Ref. 6). These results are consistent with those presented here. These additional data presented here on the nature, location, and amount of degradation are intended to lead to methods for reducing the degradation.

In the first run of Sample B, the thin edge had the lowest critical curent, and this region was limiting the current. For the second run, a short section of the thin edge was shunted with a 0.7-cm length of

Manuscript received September 30, 1986.

Contribution of NBS, not subject to copyright.

0018-9464/87/0300-1642$01.00©1987 IEEE

another cable strand. This allowed the current to get slightly higher and enabled testing of the other regions of the strand before the sample quenched. The data presented for Sample B are a combination of these two runs, not shunted and shunted.

The critical current as a function of position along the strand at 0° and 90° field angle is given in Figs. 1 and 2 for Sample A. The critical current was defined as the current at which the electric field strength was 0.1 μV/cm. The zero angle was defined as the orientation with the magnetic field parallel to the wide face of the cable. The critical current values varied by as much as 27% from the maximum at 0° and 11% at 90°. At 0° the central flat portion of the thin edge had the lowest I_c. The central flat portion of the thick edge was less degraded. The corners of both edges had a higher I_c and had some asymmetry in the same cable lay direction. This may be due to mass flow away from the cable edge during the cable fabrication. The difference between 0 and 90° is due to the effect of the conductor aspect ratio[7] and the fact that the applied magnetic field is not exactly perpendicular to the current for all portions of the strand at all angles. The cable pitch is about 17°, which would increase I_c at 0° by about 8% for the portions across the cable face.[8] At 90° the applied magnetic field is perpendicular to the cable face, but it is not perpendicular to portions of the cable edges. The major deformation direction for the cable edge is 90° from that for the cable face. The edges have their lowest I_c at 0°. The central region of the cable face does not have very much change in I_c between 0 and 90° because the strand is almost round there.

The critical current as a function of position at 0° and 90° for the Sample B is given in Figs. 3 and 4. The critical current values varied by as much as 35% from the maximum at 0° and 33% at 90°. At 0° the central flat of the thin edge had the lowest I_c, and unlike Sample A, it did not increase very much at 90°. For both samples the difference between the thin and thick edges were similar, as were the corner values. The central flat region of the thin edge is the weak link and would appear to have a degraded I_c rather than a large aspect ratio effect.[6]

A relevant question at this point is: What is the effective critical current of these strands as a function of orientation? One possibility is the current at which the average electric field strength is equal to some value (see experimental section). The effective critical current and quench current for Sample A are plotted as a function of angle in Fig. 5. The effective critical current at various electric field criteria had an angular dependence very similar to the quench current. This was not expected considering that the quench current should be strongly dominated by the degraded section (or weak link) of the strand and consequently lower at 0°. This suggests that the average E does give a relevant critical current. The end cooling around the weak link must have been sufficient such that the local heating did not have an adverse effect on I_c. The weak link at 0° contributed about 55% of the total voltage even though it only represented 5% of the total length. For the effective critical current, the weak link region is at a high electric field where the effect of a single bend is not as large (See Ref. 9 for effect of bending).

The effective critical currents and quench current for Sample B are plotted as a function of angle in Fig. 6. There are two curves without symbols. The upper was the quench current after a shunt was placed on the thin edge. The lower was the quench current before the shunt was placed on the thin edge. The lowest curve is the effective I_c at 0.1 μV/cm. The

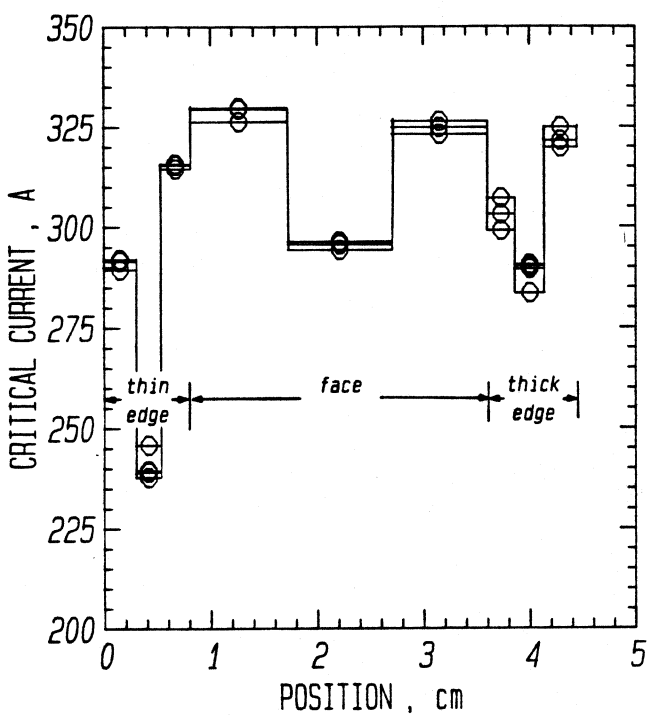

Figure 1. Sample A, I_c vs. position at 0°.

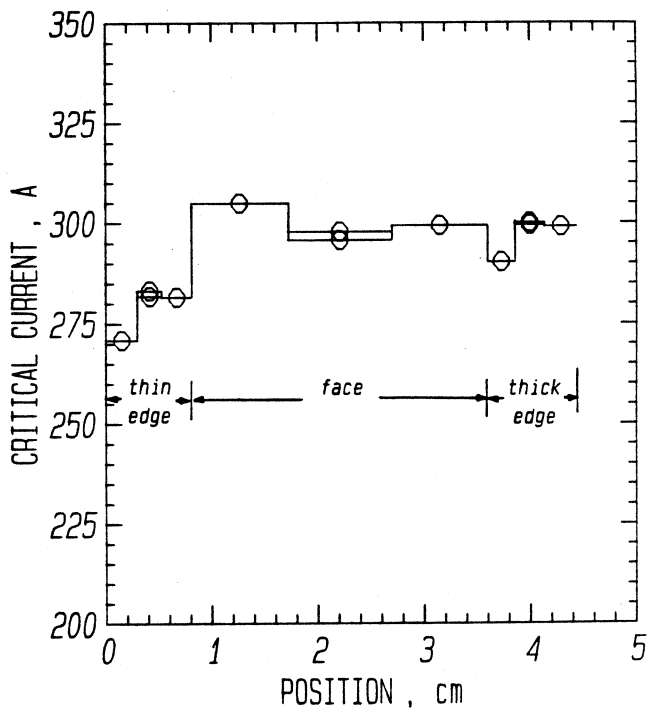

Figure 2. Sample A, I_c vs. position at 90°.

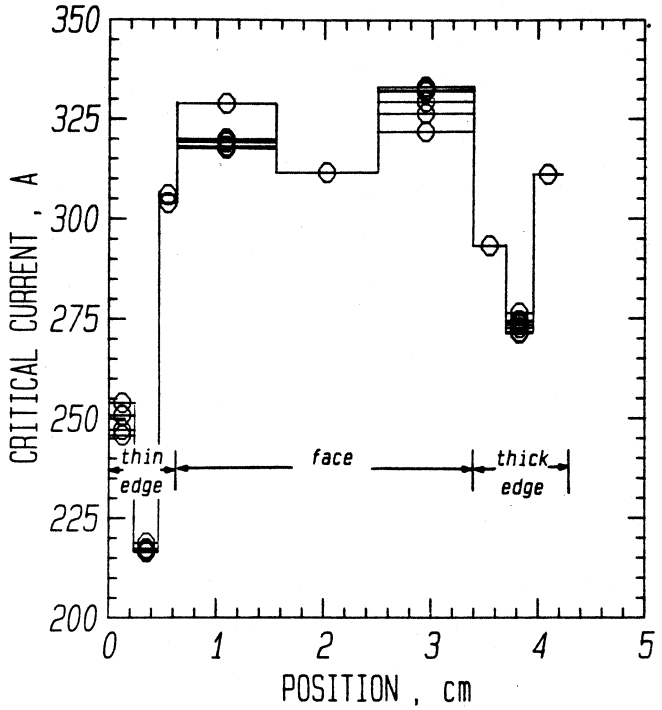

Figure 3. Sample B, I_c vs. position at 0°.

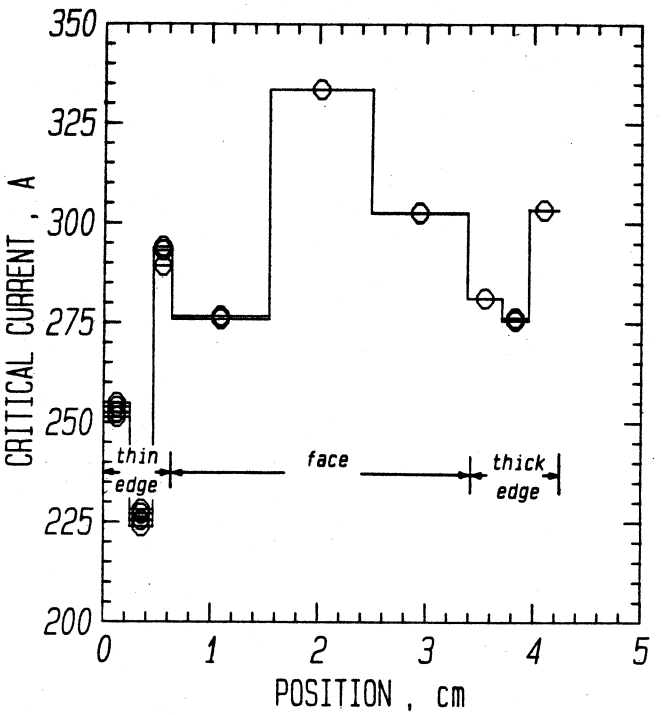

Figure 4. Sample B, I_c vs. position at 90°.

weak link at 0° contributed about 95% of the total voltage even though it represented only 5% of the total length.

Table 1 shows the percent differences of the I_c's from the starting wire (before cabling) values. The starting wire I_c's are approximate because they were measured as another part of this program in another magnet.[9] The additional lowering of the weak-link I_c for Sample B resulted in a much lower effective I_c. In fact, the difference in effective I_c's was greater than the difference in weak link I_c's at 0.1 μV/cm. At 0°, I_c of Sample B was an additional

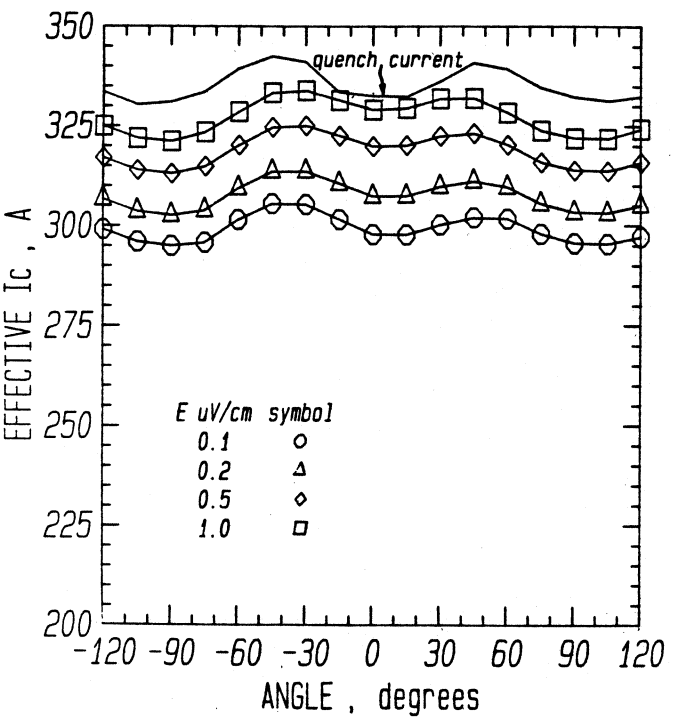

Figure 5. Sample A, effective I_c and quench I vs. angle.

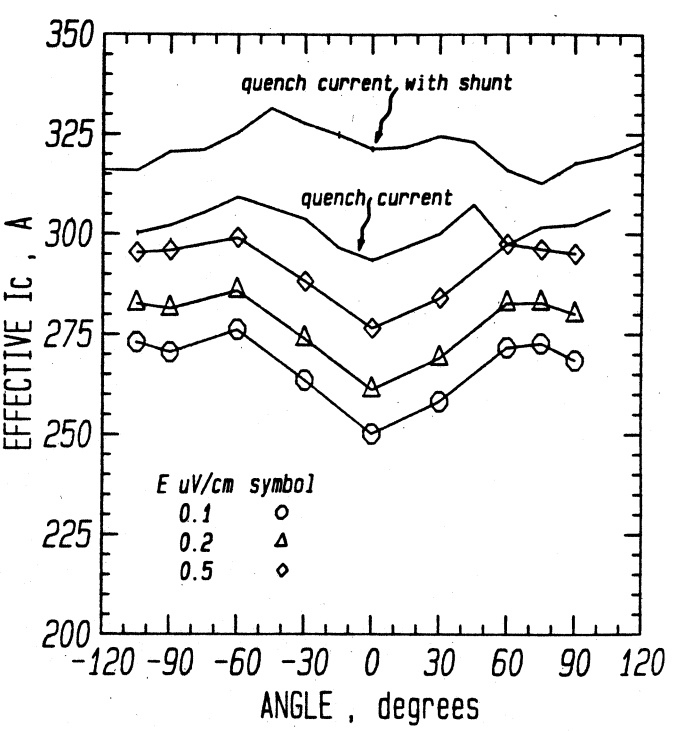

Figure 6. Sample B, effective I_c and quench I vs. angle.

Table 1. Percent differences in I_c from starting wire I_c's at 5 T, 4.0 K, and 0.1 μV/cm

Starting Wire I_c	Sample A 320 A		Sample B 347 A	
Field Angle	0°	90°	0°	90°
highest segment	+ 2.8%	- 4.7%	- 4.6%	- 4.0%
lowest segment	-25.3%	-15.3%	-37.5%	-34.9%
effective I_c	- 6.9%	- 7.5%	-27.7%	-22.8%

12% lower than that of Sample A but the effective I_c was 20% lower. The difference in I_c's at higher electric fields, however, was more than 12%. This increased effect may show that the local heating had an adverse effect on I_c for Sample B.

Discussion

Understanding the relationship between the mechanical deformation in the cabling process and the electrical performance may lead to improvements in the critical current of a cable. Comparisons of these two samples should be tempered by the fact that the starting wires were not the same but were similar enough to support the conclusions drawn from each sample. Additional current sharing that can take place in the cable will help reduce the effects of local changes in critical current. However, the experiment of shunting Sample B by soldering another strand to it (with no transport current of its own) may indicate that the best case would only be a 7% improvement. On the other hand, any compromise in end cooling could have a significant effect.

These results have two implications for short-sample critical-current testing of cables. First, the data indicate that both magnetic-field orientations need to be tested in order to determine the limiting case for the critical current. As shown above, for more degraded cables, the parallel-field case may limit. In the less degraded cables, the perpendicular case limits. The amount of degradation is not known beforehand, so both orientations need to be measured.

Second, the difference between thick and thin edge degradation shown in these data indicates that changing the direction of the test current (for each field orientation) will affect the critical current. This is because the location of the peak magnetic field changes with current direction (see Fig. 3 in Ref. 6). Thus, the peak field location relative to the thin edge should be recorded. The conservative approach in short-sample cable tests would be to make the measurement for both directions of the test current and use the critical current for the worst case. The additional measurements will help increase the understanding of cable degradation.

Conclusions

Cabling can lead to very localized reduction in critical current within a single strand. The lowest critical current was observed for the central flat part of the thin edge and this segment contributes most of the overall voltage drop. The widest spread in local critical current values along the cable strands occurs with the magnetic field perpendicular to the cable edge. Unfortunately in the dipole magnet application, this orientation is near the critical orientation. The relevant critical-current criteria for local measurements may be based on a spatial average. This is because of the extreme localization of damage, limited extent of the voltage, and strong end cooling effect which all limit the local temperature rise. Any compromise in sample stability may lower the critical current to that of the weak link.

Acknowledgements

The authors extend their thanks to S. L. Bray and W. E. Look for sample holder construction, data analysis, and plotting; J. M. Royet for samples and discussions; and R. A. Shenko for typing this paper. Research at NBS was supported by the U.S. Department of Energy, Division of High Energy Physics under Interagency Agreement No. DE-AI05-85ER40240 and research at LBL was supported by the U.S. Department of Energy, Office of Energy Sciences, Office of Energy Research under Contract No. DE-AC03-765F00098

References

1. J. W. Ekin, L. F. Goodrich, J. Moreland, E. S. Pittman, and A. F. Clark, "Electro-Mechanical Properties of Superconductors for High Energy Physics Applications," NBSIR 86-3061, National Bureau of Standards, Boulder, Colorado.

2. J. Royet and R. M. Scanlan, "Manufacture of Keystoned Flat Superconducting Cables for Use in SSC Dipoles," these proceedings, paper LB-1.

3. R. Scanlan, J. Royet, and C. E. Taylor, "Superconducting Materials for the SSC," Adv. Cryog. Eng. - Materials, Vol. 32, 697, Plenum Press, New York (1986).

4. D. C. Larbalestier, A. W. West, W. Starch, W. Warnes, P. Lee, W. K. McDonald, P. O'Larey, K. Hemachalam, B. Zeitlin, R. Scanlan, and C. Taylor, "High Critical Current Densities in Industrial Scale Composites Made From High Homogeneity Nb 46.5 Ti," IEEE Trans. on Magnetics, MAG 21, 269, 1985.

5. W. B. Sampson, Brookhaven National Laboratory., Upton, New York, private communications (1986).

6. M. Garber and W. B. Sampson, "Critical Current Anisotropy in NbTi cables," IEEE Trans. on Magnetics, MAG 21, 336, 1985.

7. L. F. Goodrich, W. P. Dube, E. S. Pittman, and A. F. Clark, "The Effect of Aspect Ratio on Critical Current in Multifilamentary Superconductors," Adv. Cryog. Eng. - Materials, Vol. 32, 833, Plenum Press, New York (1986).

8. A. F. Clark, L. F. Goodrich, F. R. Fickett, and J. V. Minervini, "Development of Standards for Superconductors, Interim Report Oct. 1980 to Jan. 1982," NBSIR 82-1678, National Bureau of Standards, Boulder, Colorado (July 1982), pp 17-36.

9. J. W. Ekin, "Critical Current vs. Stress Relationships in NbTi Superconductors," these proceedings, paper MH-6.